Electronic Supplementary Material (ESI) for Nanoscale Horizons.

Supporting Information for

Engineering Spin and Antiferromagnetic Resonances to Realize Efficient Direction-multiplexed Visible Meta-hologram

Muhammad Afnan Ansari,‡[a,b] Inki Kim,‡[c] Ivan D. Rukhlenko,[d,e] Muhammad Zubair,[a] Selcuk Yerci,*[b,f,g] Tauseef Tauqeer,*[a] Muhammad Qasim Mehmood,*[a] and Junsuk Rho*[c,h,i]

a. Department of Electrical Engineering, Information Technology University of the Punjab, Lahore 54600, Pakistan. E-mail: qasim.mehmood@itu.edu.pk, tauseef.tauqeer@itu.edu.pk

b. Department of Electrical and Electronics Engineering, Middle East Technical University, Cankaya/Ankara 06800, Turkey. E-mail: syerci@metu.edu.tr

c. Department of Mechanical Engineering, Pohang University of Science and Technology (POSTECH), Pohang 37673, Republic of Korea. E-mail: jsrho@postech.ac.kr

d. Information Optical Technologies Centre, ITMO University, Saint Petersburg 197101, Russia

e. Institute of Photonics and Optical Sciences (IPOS), School of Physics, The University of Sydney, Camperdown 2006, New South Wales, Australia

f. Department of Micro and Nanotechnology, Middle East Technical University, 06800 Çankaya/Ankara, Turkey

g. Center for Solar Energy Research and Applications, Middle East Technical University, 06800 Çankaya/Ankara, Turkey

h. Department of Chemical Engineering, Pohang University of Science and Technology (POSTECH), Pohang 37673, Republic of Korea

i. National Institute of Nanomaterials Technology (NINT), Pohang 37673, Republic of Korea

‡These authors contributed equally to this work.

Supplementary Section 1: Potential dielectric platforms

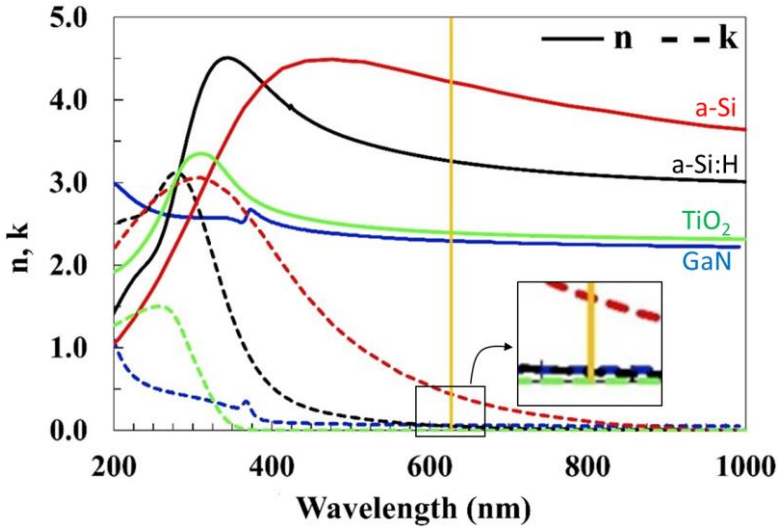

Figure S1: Ellipsometry data of potential dielectric materials in the broadband spectrum of visible light. Refractive index (solid lines) and extinction coefficient (dotted lines) spectra of conventional a-Si (red color)[1], TiO_2 (green color)[2], GaN (blue color)[3] and our a-Si:H (black color) are plotted against a broad range of wavelength (λ = 200 to 1000 nm) for comparison. A vertical solid yellow line is drawn at a wavelength of 633 nm. Measured ellipsometry data of the proposed a-Si:H shows significant reduction in the value of extinction coefficient as compared to conventional a-Si. Moreover, the higher refractive index of the a-Si:H than TiO_2 and GaN will help in achieving lower aspect ratio.

Supplementary Section 2. Direction controlled multiplexing using a-Si:H nanorods

To determine the expression of the transmitted electric field, consider the Jones matrix of a single a-Si:H nano-element with the rotation angle $\vec{\varphi}_1$ (Figure 1e) in the forward direction (T_m):

$$T_m = R(-\vec{\varphi}_1).T.R(\vec{\varphi}_1) = \begin{bmatrix} \cos\vec{\varphi}_1 & \sin\vec{\varphi}_1 \\ -\sin\vec{\varphi}_1 & \cos\vec{\varphi}_1 \end{bmatrix}\begin{bmatrix} T_{11} & 0 \\ 0 & T_{22} \end{bmatrix}\begin{bmatrix} \cos\vec{\varphi}_1 & -\sin\vec{\varphi}_1 \\ \sin\varphi_1 & \cos\vec{\varphi}_1 \end{bmatrix} =$$

$$\begin{bmatrix} T_{11}\cos^2\vec{\varphi}_1 + T_{22}\sin^2\vec{\varphi}_1 & (T_{11}-T_{22})\sin\vec{\varphi}_1\cos\vec{\varphi}_1 \\ (T_{11}-T_{22})\sin\vec{\varphi}_1\cos\vec{\varphi}_1 & T_{22}\cos^2\vec{\varphi}_1 + T_{11}\sin^2\vec{\varphi}_1 \end{bmatrix} \quad \text{(S1)}$$

Where *T* and $R(\vec{\varphi}_1)$ are the Jones matrix without rotation and the rotation operator of a-Si:H nanoelement respectively. If the incident light is LCP, then the expression of the electric field in the forward direction after passing through the proposed medium can be written as:

$$\vec{\boldsymbol{E}}_{t1} = T_m.\vec{\boldsymbol{E}}_{in} = T_m.\vec{\boldsymbol{E}}_L = \frac{1}{\sqrt{2}}\begin{bmatrix} T_{11}\cos^2\vec{\varphi}_1 + T_{22}\sin^2\vec{\varphi}_1 & (T_{11}-T_{22})\sin\vec{\varphi}_1\cos\vec{\varphi}_1 \\ (T_{11}-T_{22})\sin\vec{\varphi}_1\cos\vec{\varphi}_1 & T_{22}\cos^2\vec{\varphi}_1 + T_{11}\sin^2\vec{\varphi}_1 \end{bmatrix}\begin{bmatrix}1\\ i\end{bmatrix} \quad \text{(S2)}$$

$$\vec{\boldsymbol{E}}_{t1} = \frac{T_{11}+T_{22}}{2}.\vec{\boldsymbol{E}}_L + \frac{T_{11}-T_{22}}{2}e^{i2\vec{\varphi}_1}.\vec{\boldsymbol{E}}_R \quad \text{(S3)}$$

$$\vec{\boldsymbol{E}}_{t2} = \frac{T_{11}+T_{22}}{2}.\vec{\boldsymbol{E}}_L + \frac{T_{11}-T_{22}}{2}e^{i2\vec{\varphi}_2}.\vec{\boldsymbol{E}}_R \quad \text{(S4)}$$

$\boldsymbol{E}_{t1}$ and $\boldsymbol{E}_{t2}$ are the scattered electric fields from first and second nanoelements in the supercell, respectively. According to Equations S3 and S4, the phase of the cross-polarized component depicts linear dependency on the rotation angle of the nanoelement with a factor of 2. Similarly, expressions of total electric fields transmitted from a supercell (Figure 1e) containing two nanoelements with shifted rotation angles can be written as:

$$\vec{\boldsymbol{E}}_t = \vec{\boldsymbol{E}}_{t1} + \vec{\boldsymbol{E}}_{t2} = \left[\frac{T_{11}+T_{22}}{2}.\vec{\boldsymbol{E}}_L + \frac{T_{11}-T_{22}}{2}e^{i2\vec{\varphi}_1}.\vec{\boldsymbol{E}}_R\right] + \left[\frac{T_{11}+T_{22}}{2}.\vec{\boldsymbol{E}}_L + \frac{T_{11}-T_{22}}{2}e^{i2\vec{\varphi}_2}.\vec{\boldsymbol{E}}_R\right], \quad \text{(S5)}$$

$$\overleftarrow{\boldsymbol{E}}_t = \overleftarrow{\boldsymbol{E}}_{t1} + \overleftarrow{\boldsymbol{E}}_{t2} = \left[\frac{T_{11}+T_{22}}{2}.\overleftarrow{\boldsymbol{E}}_L + \frac{T_{11}-T_{22}}{2}e^{i2\overleftarrow{\varphi}_1}.\overleftarrow{\boldsymbol{E}}_R\right] + \left[\frac{T_{11}+T_{22}}{2}.\overleftarrow{\boldsymbol{E}}_L + \frac{T_{11}-T_{22}}{2}e^{i2\overleftarrow{\varphi}_2}.\overleftarrow{\boldsymbol{E}}_R\right], \quad \text{(S6)}$$

The bold letters indicate vector quantities; however, the top arrows only correspond to the direction i.e., forward or backward. Where $\vec{\varphi}_1$ and $\overleftarrow{\varphi}_1$ are the rotation angles associated with first nanoelements in the supercell for the forward and backward directions, respectively. Similarly, $\vec{\varphi}_2$ and $\overleftarrow{\varphi}_2$ denote the rotation angles of the second nanoelement in the supercell for the forward and backward directions, respectively, as shown in Figure 1e. Numerical optimization and simulations not only verified the linear dependency but also insured the maximum value of the cross-polarized component. Therefore the co-polarized components of transmitted electric fields (1st and 3rd terms) are small and can be neglected.

$$\vec{\boldsymbol{E}}_t \approx \frac{T_{11}-T_{22}}{2}e^{i2\vec{\varphi}_1}.\vec{\boldsymbol{E}}_R + \frac{T_{11}-T_{22}}{2}e^{i2\vec{\varphi}_2}.\vec{\boldsymbol{E}}_R \quad \text{(S7)}$$

$$\overleftarrow{\boldsymbol{E}}_t \approx \frac{T_{11}-T_{22}}{2}e^{i2\overleftarrow{\varphi}_1}.\overleftarrow{\boldsymbol{E}}_R + \frac{T_{11}-T_{22}}{2}e^{i2\overleftarrow{\varphi}_2}.\vec{\boldsymbol{E}}_R \quad \text{(S8)}$$

Supplementary Section 3. Fabrication of metasurfaces

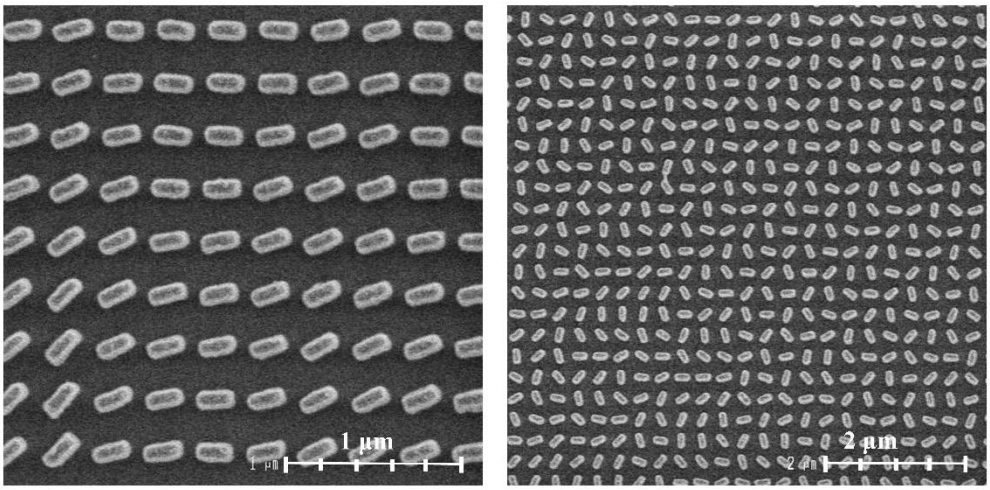

Figure S2. Scanning electron microscope (SEM) images of partial regions of fabricated direction-controlled metasurface hologram. Each a-Si:H nano-elements (200 nm x 80 nm) represent a unique phase pixel defined in the direction-controlled metasurface. The scale bars of left and right images are 1 μm and 2 μm, respectively. The size of equivalent pixel is 290 x 290 nm^2.

The device is fabricated on a substrate made up of fused silica (SiO_2) having a thickness of 500 μm. Using plasma enhanced chemical vapor deposition (PECVD, BMR Technology HiDep-SC), hydrogenated amorphous silicon with 380 nm height is deposited. The deposition is controlled at a rate of 1.3 nm/s at 300 °C with a flow rate of SiH_4 and H_2 gasses equal to 10 and 75 sccm respectively. The positive resist is spin coated with a speed of 2000 rpm for 60 s and baked on the hotplate for five minutes at a temperature of 180 degrees centigrade. The final thickness of resist is 100 nm. The dielectric substrate has charging effect, therefore, to avoid this effect, prior to the exposure to e-beam we have used a layer of conductive polymer named as Showa Denko, E-spacer 300Z via spin coating at a speed of 2000 rpm for 60 s. The desired nanorod patterns are transferred onto a positive resist (Microchem, 495 PMMA A2) by e-beam lithography (ELIONIX, ELS–7800, 80 kV, 50 pA). The amount of e-beam exposure is approximately equal to 1,280~1,600 μC/cm^2. DI water is used to remove the layer of a conductive polymer after the e-beam exposure. The development of PMMA resist carried out in a 1:3 solution of methyl isobutyl ketone ($C_6H_{12}O$) / isopropyl alcohol ($CH_3CHOHCH_3$) for twelve minutes at a temperature of 0 °C. After the development of PMMA resist, the sample is washed for 30 s by isopropyl alcohol. Using e-beam evaporation (KVT, KVE–ENS4004), 30 nm-thick chromium is deposited and lift-offed for ten minutes in hot acetone (50 °C). The fabricated chromium nanorod structures are used as etch mask, and

uncovered Si is removed using dry etching (DMS, silicon/metal hybrid etcher). At last, by using Chromium etchant (CR-7), the remaining Chromium mask is removed.

Supplementary Section 4: Technology overview

A highly efficient Huygens' metasurface was developed for the near-infrared domain using silicon nanodisks with 99% transmission efficiency[4]. Advancement in the visible domain was made by designing a metahologram for three primary colors using geometric silicon nanoelements with a measured efficiency of 13.2%, 11.1% and 8.9% for red, green and blue light, respectively[5]. The limitation of the transparency window of silicon at the infrared domain became the motivation to explore new materials and novel nanofabrication techniques to extend the operation of dielectric metadevices to the visible domain. A highly efficient metahologram was fabricated using atomic layer deposition of TiO_2 with absolute efficiency greater than 78%[6]. Similarly, extremely efficient GaN-based metalenses are produced with the highest efficiency of 91.6% at an operation wavelength of 532 nm[7]. However, the fabrication methods of TiO_2 and GaN-based metadevices are very complex and expensive due to their larger aspect ratio requirements (12 to 17.7) to achieve full phase coverage[6, 7]. Therefore, we have presented a direction-multiplexed metahologram using a-Si:H for the first time in the transmission mode with antiferromagnetic resonance modes underpinning the high conversion efficiency of cross-polarized component (61%) in the visible domain with manufactural ease due to a substantial decrease in the aspect ratio (up to 4.7). The proposed design and methodology is suitable for practical applications and large scale production due to its cost-effectiveness and compatible fabrication process with already mature semiconductor foundries.

Table S1

References	*Material*	*Max. Aspect Ratio*	*Device*	*Wavelength*	*Efficiency (%)*
Manuel Decker et al., Adv. Optical Mater. 2015 [4]	Si	~1	Huygens' Metasurface	NIR	99
Wenyu Zhao et al., Optics Letters. 2016 [5]	Si	2	Metahologram	Red, Green and Blue	13.2, 11.1 and 8.9
Robert C. Devlin et al., PNAS. 2016 [6]	TiO_2	15	Metahologram	Visible	78
Bo Han Chen et al., Nano Letters. 2017 [7]	GaN	12	Metalens	Red, Green, Blue	50.6, 91.6, and 87
Shuming Wang et al. Nature Nanotechnology. 2018 [8]	GaN	17.7	Achromatic Metalens	400 to 660 nm	40
This work	a-Si:H	4.7	Metahologram	633 nm	61

Supplementary References

1 D. Pierce, W. Spicer, Phys. Rev. B 1972, 5, 3017-3029.

2 T. Siefke, S. Kroker, K. Pfeiffer, O. Puffky, K. Dietrich, D. Franta, I. Ohlídal, A. Szeghalmi, E.-B. Kley, A. Tünnermann, Adv. Opt. Mater. 2016, 4, 1780-1786.

3 T. Kawashima, H. Yoshikawa, S. Adachi, S. Fuke, K. Ohtsuka, J. Appl. Phys. 1997, 82, 3528.

4 Decker M, Staude I, Falkner M, Dominguez J, Neshev D N, Brener I, Pertsch T and Kivshar Y S 2015 High-Efficiency Dielectric Huygens' Surfaces Adv. Opt. Mater.

5 Zhao W, Liu B, Jiang H, Song J, Pei Y and Jiang Y 2016 Full-color hologram using spatial multiplexing of dielectric metasurface Opt. Lett.

6 Devlin R C, Khorasaninejad M, Chen W T, Oh J and Capasso F 2016 Broadband high-efficiency dielectric metasurfaces for the visible spectrum Proc. Natl. Acad. Sci. 113 10473–8

7 Chen B H, Wu P C, Su V C, Lai Y C, Chu C H, Lee I C, Chen J W, Chen Y H, Lan Y C, Kuan C H and Tsai D P 2017 GaN Metalens for Pixel-Level Full-Color Routing at Visible Light Nano Lett.

8 Wang S, Wu P C, Su V C, Lai Y C, Chen M K, Kuo H Y, Chen B H, Chen Y H, Huang T T, Wang J H, Lin R M, Kuan C H, Li T, Wang Z, Zhu S and Tsai D P 2018 A broadband achromatic metalens in the visible Nat. Nanotechnol.